Title

Individual differences in children's global motion sensitivity correlate with TBSS-based measures of the superior longitudinal fasciculus

Authors

Braddick, Oliver
Atkinson, Janette
Akshoomoff, Natacha
et al.

Publication Date

2017-12-01

DOI

10.1016/j.visres.2016.09.013

Peer reviewed

Vision Research 141 (2017) 145–156

Contents lists available at ScienceDirect

Vision Research

journal homepage: www.elsevier.com/locate/visres

Individual differences in children's global motion sensitivity correlate with TBSS-based measures of the superior longitudinal fasciculus

Oliver Braddick [a,*], Janette Atkinson [a,b], Natacha Akshoomoff [c,d], Erik Newman [c,d], Lauren B. Curley [c,g], Marybel Robledo Gonzalez [c,g], Timothy Brown [f,h], Anders Dale [e,f,g,h], Terry Jernigan [c,d,e,g]

[a] Department of Experimental Psychology, University of Oxford, UK
[b] Faculty of Brain Sciences, University College London, UK
[c] Center for Human Development, University of California San Diego, CA, USA
[d] Department of Psychiatry, University of California San Diego, La Jolla, CA, USA
[e] Department of Radiology, University of California San Diego, La Jolla, CA, USA
[f] Department of Neurosciences, University of California San Diego, La Jolla, CA, USA
[g] Department of Cognitive Science, University of California San Diego, La Jolla, CA, USA
[h] Department of Multimodal Imaging Laboratory, University of California San Diego, La Jolla, CA, USA

ARTICLE INFO

Article history:
Received 1 July 2016
Received in revised form 20 September 2016
Accepted 22 September 2016
Available online 16 December 2016

Keywords:
Individual differences
Visual brain development
Global motion sensitivity
Global form sensitivity
Fractional anisotropy
Superior longitudinal fasciculus

ABSTRACT

Reduced global motion sensitivity, relative to global static form sensitivity, has been found in children with many neurodevelopmental disorders, leading to the "dorsal stream vulnerability" hypothesis (Braddick et al., 2003). Individual differences in typically developing children's global motion thresholds have been shown to be associated with variations in specific parietal cortical areas (Braddick et al., 2016). Here, in 125 children aged 5–12 years, we relate individual differences in global motion and form coherence thresholds to fractional anisotropy (FA) in the superior longitudinal fasciculus (SLF), a major fibre tract communicating between parietal lobe and anterior cortical areas. We find a positive correlation between FA of the right SLF and individual children's sensitivity to global motion coherence, while FA of the left SLF shows a negative correlation. Further analysis of parietal cortical area data shows that this is also asymmetrical, showing a stronger association with global motion sensitivity in the left hemisphere. None of these associations hold for an analogous measure of global form sensitivity. We conclude that a complex pattern of structural asymmetry, including the parietal lobe and the superior longitudinal fasciculus, is specifically linked to the development of sensitivity to global visual motion. This pattern suggests that individual differences in motion sensitivity are primarily linked to parietal brain areas interacting with frontal systems in making decisions on integrated motion signals, rather than in the extra-striate visual areas that perform the initial integration. The basis of motion processing deficits in neurodevelopmental disorders may depend on these same structures.

1. Introduction

Recent studies of individual differences in measures of visual performance have proved informative for exploring the structure of visual processes (e.g. Goodbourn et al., 2012; Peterzell, 2016). Further insights may be gained by relating these differences in performance to variations in brain structure. The brains of individual children, while following clear common developmental pathways in terms of regional cortical area, thickness, and white matter development, also show marked individual differences in all these measures (e.g. Brown, 2016). Such variations have been correlated with individual differences in behavioral and cognitive function, for example in executive function (Fjell et al., 2012), anxiety (Newman et al., 2015) or intelligence (Fjell et al., 2015). Using this approach with visual perceptuo-cognitive functions, we can consider what brain structures constrain aspects of visual performance in development.

Here we examine structural correlates of children's performance in the detection of global visual motion, a function

Abbreviations: TBSS, tract-based spatial statistics; FA, fractional anisotropy; SLF, superior longitudinal fasciculus; FNIRT, FMRIB nonlinear image registration tool; MNI, Montreal Neurological Institute; IPS, intraparietal sulcus; TMS, transcranial magnetic stimulation.

* Corresponding author at: Dept. of Experimental Psychology, University of Oxford, South Parks Road, Oxford OX1 3UD, UK.
E-mail address: oliver.braddick@psy.ox.ac.uk (O. Braddick).

http://dx.doi.org/10.1016/j.visres.2016.09.013
0042-6989/

dependent on extra-striate processing in the dorsal cortical stream. Global motion sensitivity develops through middle childhood, more slowly than the analogous measure for global static form, with considerable variation between individual children and a dependence on spatio-temporal parameters (for example, Atkinson & Braddick, 2005; Gunn et al., 2002; Hadad, Daphne Maurer, & Lewis, 2011; Meier & Giaschi, 2014). We have developed child-friendly tests providing comparable measures of global motion and global form, first testing sensitivity for translational motion ('The Road in the Snowstorm'; Atkinson et al., 1997; Gunn et al., 2002) and in a subsequent version with rotary motion matching form and motion stimuli more closely ('Find the Ball in the Grass'; Atkinson & Braddick, 2005). Fig. 1 illustrates the form and motion components of the 'Find the Ball in the Grass' test).

Global motion sensitivity is specifically impaired, compared to global form, in a range of genetic and acquired developmental disorders, summarized in Table 1, leading us to propose the hypothesis of 'dorsal stream vulnerability' (Atkinson et al., 1997; Braddick & Atkinson, 2011; Braddick, Atkinson, & Wattam-Bell, 2003; Atkinson, in press). These disorders show other deficits of visuo-motor function, spatial cognition, and attention, associated with the functions of the dorsal stream (Atkinson & Braddick, 2011; Kravitz, Saleem, Baker, & Mishkin, 2011). Understanding the brain correlates of global motion sensitivity, therefore, should help us understand the developmental constraints on these functions and suggest structures that may be associated with its vulnerability in developmental disorders.

The opportunity to address these questions comes from an extensive study of a group of children, aged from 5 to 12 years, who underwent multimodal brain imaging and extensive behavioral assessment, including measurement of global form and motion thresholds, in the PLING study (Pediatric Longitudinal Imaging, Neurocognition & Genetics) (Akshoomoff et al., 2014; Brown et al., 2012; Fjell et al., 2012; Jernigan et al., 2016; see http://www.chd.ucsd.edu/research/pling.html) at the University of California, San Diego. We have already reported results from initial analyses on regional measurements of cortical area in this group, which show that good individual performance on a test of global motion sensitivity is associated with relative enlargement of the parietal lobe, especially in the region of the intraparietal sulcus, and relatively smaller area of the occipital lobe (Atkinson et al., 2014; Braddick et al., 2016). Global motion sensitivity was also correlated with performance on mathematical cognition and visuo-motot integration. Here we extend this analysis to individual differences in fractional anisotropy (FA) in white matter fibre tracts and extend our analysis of regional measurements of cortical areas.

Specifically, we test the hypothesis that individual differences in children's global motion performance are associated with individual differences in FA in the superior longitudinal fasciculus (SLF), a major fibre bundle with extensive connections in the parietal lobe and providing two-way communication with frontal and prefrontal areas, including supplementary motor and premotor areas (Kamali, Flanders, Brody, Hunter, & Hasan, 2014). Given the relationship of global motion sensitivity to parietal area, we expect that this tract may play an important role in transmitting motion information to anterior cortical areas, and perhaps in top-down modulation of motion processing in parietal and extra-striate areas. It is possible that such modulation, a form of attentional control, may play a significant role in individual abilities to detect global motion. There is long-standing evidence that spatial attention has a lateralized brain basis in the right hemisphere (e.g. Mesulam, 1981) and more specifically, parieto-frontal attentional networks, including the superior longitudinal fasciculus, are known to be lateralized (e.g. Szczepanski, Konen, & Kastner, 2010; Thiebaut de Schotten et al., 2011). We therefore examined relations with the right and left superior longitudinal fasciculi included separately in our statistical models.

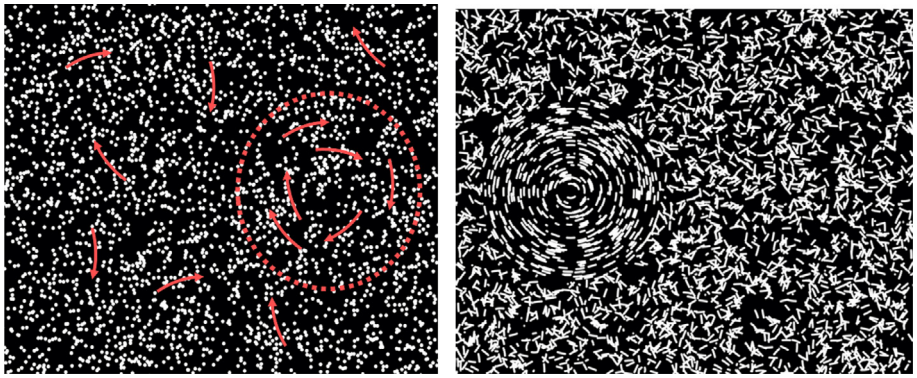

Fig. 1. Schematic illustration of the stimuli used in the 'Find the Ball in the Grass' tests, shown at 100% coherence. Left: stimulus for motion coherence testing, with the target shown on the right. Right: stimulus for form coherence testing, with the target shown on the left.

Table 1
Neurodevelopmental disorders showing global motion sensitivity impaired relative to global form sensitivity.

Disorder group	Origin	References
Young Williams Syndrome children	Genetic	Atkinson et al. (1997), Atkinson, Braddick, Anker, Curran, and Andrew (2003)
Adult Williams Syndrome	Genetic	Atkinson et al. (2006)
Autism	Possibly genetic	Spencer et al. (2000), Simmons et al. (2009)
Hemiplegic children	Acquired	Gunn et al. (2002)
Developmental dyslexia	?	Hansen, Stein, Orde, Winter, and Talcott (2001)
Fragile X	Genetic	Kogan et al. (2004)
Very preterm born	Acquired	Atkinson and Braddick (2007), Taylor, Jakobson, Maurer, and Lewis (2009)
Congenital cataract	Acquired?	Compare Ellemberg, Lewis, Maurer, Brar, and Brent (2002) with Lewis et al. (2002)
Strabismic amblyopia	Acquired?	Simmers, Ledgeway, and Hess (2005), Ho et al. (2005)

2. Methods

2.1. Participants

The participants were drawn from a sample of children making their first visits for data collection in the PLING study at the University of California, San Diego (UCSD). In addition to measurements of global form and motion sensitivity, participants completed an extensive battery of cognitive tests, as well as a structural magnetic resonance imaging (MRI) session in which diffusion-weighted images were acquired. The work was carried out in accordance with the Code of Ethics of the World Medical Association (Declaration of Helsinki) and the human research protections program and institutional review board at UCSD approved all experimental and consenting procedures. Written parental informed consent was obtained for all participants and child assent from those 7 years and older. Participants were screened for history of major developmental, psychiatric, or neurological disorders, brain injury, or other medical conditions that affect development. Only participants aged between 5:0 and 12:11 years, who completed two measurements of both global motion and global form sensitivity, with neuroimaging data including fractional anisotropy images that passed a quality check, were included.

Data are presented from 125 children whose diffusion-weighted imaging data met the quality control criteria, a subset of the 154 whose cortical area measurements were analyzed in Braddick et al. (2016). They included 66 males and 59 females, mean age 7.53 yr (s.d. = 1.76 yr); numbers in each 1-year band were: 5+ yr + N = 31; 6+ yr + N = 23; 7+ yr + N = 18; 8+ yr + N = 27; 9+ yr + N = 13; 10+ yr + N = 13.

2.2. Global form and motion testing: the 'Find the ball in the grass' test

Global motion and form thresholds were determined as the minimum percentage of coherently organized elements, embedded among random noise elements, for which children could detect global structure. The test was similar to that of Gunn et al. (2002) but with concentric stimulus displays (Atkinson & Braddick, 2005) on a laptop computer screen, designed to make the form and motion tasks as comparable as possible. Participants had to report whether a circular region, 'the Ball', containing concentrically organized short arcs or trajectories of moving dots, appeared on the left or right of center in a background of randomly oriented elements.

The display subtended 25 × 18 deg arc at the viewing distance of 50 cm. The *global motion* display contained 3000 dots each 11 min arc diameter, moving at 4.1 deg/s. Each dot had a lifetime of 8 frames (133 ms) after which it disappeared from the screen. Within the circular target region (the "Ball"), diameter 9.5 deg arc centered 6.3 deg left or right of screen center, coherent dots moved in concentric circular paths. The percentage of dots sharing this coherent motion varied from trial to trial as described below. The remaining dots within this region, and all the dots elsewhere on the screen, moved in randomly oriented arcs whose curvature followed the same distribution as the population of coherently moving dot trajectories.

The *global form* display contained 3000 stationary arc segments, each 8 min arc wide × 42 min arc long. Within the same circular "Ball" regions as in the global motion display, the coherent arcs were oriented to be concentric. The percentage of arcs sharing this coherent alignment varied according to the same adaptive procedure as for motion. The remaining arcs within this region, and all the arcs elsewhere on the screen, were randomly oriented arcs with the same distribution of curvature as the coherently oriented arcs. Both displays are illustrated in Fig. 1.

Participants completed four test runs, alternating runs with the global form and the global motion display, with the starting test randomized across participants. On each trial, the structured "Ball" region was presented randomly on the left or right of center, and the child was asked to point to the side that contained the "Ball" (circular pattern), or, for older children, to press the corresponding arrow key on the keyboard. The display terminated if the child had not responded within 10 s, although most responses were made in the first few seconds. The child's response terminated the trial. Each run began with coherence fixed at 100%, and these trials were continued until the tester was satisfied that the child understood the task. In the following test phase, the coherence level of the target region was varied according to the *Psi* adaptive procedure (Kontsevich & Tyler, 1999) which uses a Bayesian approach to place each trial at the point where it will give the most information about the 2-dimensional posterior probability distribution of the threshold and slope of the psychometric function. The estimated threshold was the mean threshold from this distribution, after the completion of 30 trials. Since the adaptive procedure leads to difficult decisions as stimuli are delivered increasingly close to the individual's threshold, the children's motivation was maintained by delivering an easily visible stimulus (100% coherence) on every sixth trial. In over 95% of occasions, the responses to these 'catch' trials was correct; when it was not correct the child was reminded to indicate the side containing the circular pattern. No children were eliminated for repeated errors on these 'catch' trials.

The thresholds used in analysis were the mean of two values from a child's two test runs with the specific stimulus (global motion or global form).

2.3. Neuroimaging and analysis: MRI scanning protocol

The neuroimaging protocol was as described in Jernigan et al. (2016). A standardized multiple-modality high-resolution structural MRI protocol was implemented, involving 3D T1-weighted volumes and a set of diffusion-weighted scans, on a GE 3T Signa HDx scanner and a 3T Discovery 750x scanner (GE Healthcare) using eight-channel phased array head coils. The protocol included a conventional three-plane localizer, a sagittal 3D inversion recovery spoiled gradient echo T1-weighted volume optimized for maximum gray/white matter contrast (echo time = 3.5 ms, repetition time = 8.1 ms, inversion time = 640 ms, flip angle = 8°, receiver bandwidth = ± 31.25 kHz, FOV = 24 cm, frequency = 256, phase = 192, slice thickness = 1.2 mm), and two axial 2D diffusion tensor imaging (DTI) pepolar scans (30-directions b-value = 1000, TE = 83 ms, TR = 13,600 ms, frequency = 96, phase = 96, slice thickness = 2.5 mm, FOV = 24 cm).

2.4. Analysis of fractional anisotropy of white matter

Our methods for defining fractional anisotropy (FA) of the superior longitudinal fasciculus followed closely those of Vestergaard et al. (2011). All fibre tracts were spatially normalized and aligned across all subjects using tract-based spatial statistics (Smith et al., 2006), a module in FSL 5.0.2 (Smith et al., 2004). The FA images of all subjects were aligned into a common space by implementing the non-linear registration tool FNIRT (Andersson et al., 2007a, 2007b). Next, a subset group of 50 participants were selected to be representative of the whole group matched in distribution of age and sex. For these 50 participants, all FA images were non-linearly registered to the FA images of every other subject within this group, in order to find the group's most representative FA image. Using affine registration, the most representative FA image was then aligned to MNI space and subsequently the subset of 50 participants were aligned to this image and transformed into

1 mm^3 MNI space. The mean FA image for the subset group of 50 participants was created, and formed the study-specific target to which the entire dataset was aligned, and transformed into 1 mm^3 MNI space. Next, a cross-subject mean FA image from the entire dataset was created and thinned to generate the mean FA skeleton for the entire dataset, representing the centers of all tracts common to the group. The mean FA skeleton for the entire dataset was thresholded at FA > 0.2 and contained approximately 119,017 1 mm^3 interpolated voxels. All participants' aligned FA data were then projected onto this skeleton, by locating the voxels with the highest local FA value in the direction perpendicular to the tracts in the skeleton and assigning this value to the subject's skeleton at the given standardized location. Such projection yields a mapping of each voxel location in the skeleton to a specific voxel in the individual participants' FA maps. This process accounts for residual misalignments between individuals after the initial registration, and minimizes any systematic between-participants differences in tract location. An eigenvalue color-coded map corresponding to the target FA map was created by applying the affine transformation generated when aligning the most representative FA image to MNI space to corresponding primary eigenvector (v_1) image using the FSL "vecreg" command.

The superior longitudinal fasciculus region-of-interest (ROI) was delimited for both the left and right hemisphere on the mean FA skeleton overlaid on the target FA map. It was defined using the color-coded target FA map in accordance with the MRI atlas from Mori, Wakana, Nagae-Poetscher, and van Zijl (2005). The SLF ROI contained the "stalk" or core of the tract, which extended from superior parietal cortex to dorsolateral prefrontal cortex, and limited to voxels with anterior-posterior oriented primary eigenvectors. Of the distinct branches of the SLF (Makris et al., 2005), it corresponds most closely to SLF II, although it tends to exclude angled or bending fibres because of the restriction to anterior-posterior eigenvectors. Fig. 2 illustrates the region of interest so defined. The left SLF contained 577 voxels and the right SLF contained 522 voxels. The mean FA within each region of interest was extracted for both the left and the right SLF as well as whole skeleton FA, an estimate of global white matter FA, for all participants. The mean FA in the bilateral SLF was found to be normally distributed across participants (W = 0.99, p-value = 0.84 on the Shapiro-Wilk normality test).

2.5. Area measures of individual cortical lobes

Results reported here for relation to cortical area were obtained from the procedures described in Braddick et al. (2016). In particular the areas of the occipital and parietal lobes were defined from a genetically informed, cortical parcellation scheme, which used a fuzzy clustering method to analyze the matrix of genetic correlations among vertex-wise estimates of cortical surface expansion in a sample of monozygotic and dizygotic twins (Chen et al., 2012).

2.6. Statistical analysis

The relationships between the visual performance measures of global form and motion, and the anatomical measures of fractional anisotropy and of lobe area, were analyzed by multiple regression models fitted by a least-squares criterion using the software package JMP Pro 12 (SAS Institute, Cary NC). Children's global motion thresholds or global form thresholds were used as the dependent variable, with age, age^2, gender, and MRI scanner as predictors, as well as the anatomical measures of interest. These analyses yielded tables of parameter estimates with t-values and significance levels for each effect: examples of these are presented in Tables 2–5.

To explore the spatial distribution of relationships beyond the hypothesised link between SLF and global motion, separate effect size maps were also constructed, showing the t-value of the corre-

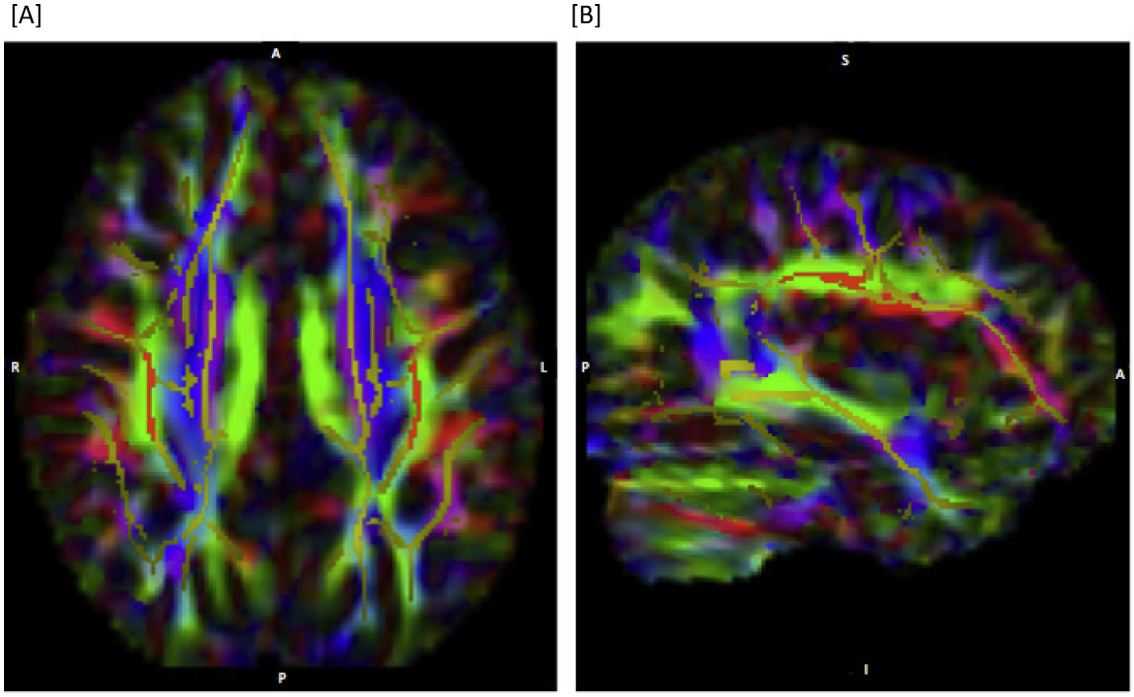

Fig. 2. Depiction of region of interest defined for the superior longitudinal fasciculus (SLF). [A] Depicts an axial slice at MNI co-ordinate z = 36; [B] depicts a sagittal slice of the right hemisphere at x = 37. The images show the mean FA skeleton in yellow, overlaid on the color-coded DTI maps where green indicates diffusion in the anterior-posterior direction, blue in the inferior-superior direction, and red in a lateral direction. The red region superimposed on the skeleton is the defined region of interest (anterior-posterior diffusion was one of the criteria used- see text).

Table 2
Regression models for motion and form coherence thresholds against fractional anisotropy (FA) in left and right superior longitudinal fasciculus (SLF). Note that a negative t-value signifies a positive association with high sensitivity to global motion or form. Bold type indicates significance $p \leqslant 0.05$.

	Motion coherence threshold		Form coherence threshold	
Term	t ratio	p > |t|	t ratio	p > |t|
Intercept	4.98	**<0.0001******	2.07	**0.040***
Age	−7.75	**<0.0001******	−4.34	**<0.0001******
Age * age	3.57	**<0.0005*****	1.99	**0.049***
Gender	0.34	0.733	0.30	0.765
Left SLF FA	2.43	**0.017***	0.45	0.652
Right SLF FA	−2.99	**0.003****	0.10	0.917

**** $p \leqslant 0.0001$.
*** $p \leqslant 0.001$.
** $p \leqslant 0.01$.
* $p \leqslant 0.05$.

Table 3
Regression model for motion coherence thresholds against fractional anisotropy (FA) in left and right superior longitudinal fasciculus (SLF) and in the overall white matter skeleton. Note that a negative t-value signifies a positive association with high sensitivity to global motion or form. Bold type indicates significance $p \leqslant 0.05$.

	Motion coherence threshold	
Term	t ratio	p > |t|
Intercept	3.14	**<0.0021****
Age	−6.72	**<0.0001******
Age * age	3.56	**<0.0005*****
Gender	0.15	0.881
Left SLF FA	2.54	**0.012***
Right SLF FA	−2.59	**0.011****
Total skeleton FA	−0.83	**0.406**

**** $p \leqslant 0.0001$.
*** $p \leqslant 0.001$.
** $p \leqslant 0.01$.
* $p \leqslant 0.05$.

Table 5
Regression models for motion coherence thresholds against FA of left and right SLF, and bilateral parietal area. Note that a negative t-value signifies a positive association with high sensitivity to global motion. Bold type indicates significance $p \leqslant 0.05$.

Term	t ratio	Prob > |t|
Intercept	5.7	**<0.0001******
Age	−7.78	**<0.0001******
Age * age	4.00	**0.0001******
Gender	−1.14	0.258
Bilateral parietal area	−2.57	**0.011***
Right SLF FA	−2.76	**0.0068****
Left SLF FA	2.49	**0.014***

**** $p \leqslant 0.0001$.
** $p \leqslant 0.01$.
** $p \leqslant 0.05$.

lations between global motion thresholds and FA, and global form thresholds and FA, adjusted for age, age^2, and gender. The t-maps were generated in FSL using whole brain linear regression across the whole skeleton with the global motion measure, age, age^2, and gender as predictors and FA as the dependent variable. Voxel level t-value ranges for both positive and negative correlations ($df = 120$), uncorrected for multiple comparisons, are indicated by a color code described in the legend for Fig. 6.

3. Results

3.1. Motion and form coherence thresholds as a function of age

As expected, there was a marked improvement over the age range of this sample in sensitivity both to global form and to global motion. Data from the present sample are illustrated in Fig. 3. In line with earlier findings (Atkinson & Braddick, 2005; Braddick et al., 2016; Gunn et al., 2002), these measurements showed a stee-

Table 4a
Regression models for motion coherence thresholds against area of the left occipital and left parietal cortical lobes, with total cortical area of the left hemisphere included in the model. Note that a negative t-value signifies a positive association with high sensitivity to global motion or form. Bold type indicates significance $p \leqslant 0.05$.

Term	t ratio	p > |t|		t ratio	p > |t|
Intercept	7.04	**<0.0001******		7.46	**<0.0001******
Age	−7.30	**<0.0001******		−8.06	**<0.0001******
Age * age	3.81	**0.0002*****		3.95	**0.0001******
Gender	−0.92	0.359		−0.87	0.384
L occipital area	2.45	**0.016***	L parietal area	−2.14	**0.0348***
L total cortical area	−3.18	**0.0019****	L total cortical area	1.24	0.219

**** $p \leqslant 0.0001$.
*** $p \leqslant 0.001$.
** $p \leqslant 0.01$.
* $p \leqslant 0.05$.

Table 4b
As Table 4a, but regression models for motion coherence thresholds against cortical areas in the right hemisphere.

term	t ratio	p > |t|		t ratio	p > |t|
Intercept	7.12	**<0.0001******		7.38	**<0.0001******
Age	−7.61	**<0.0001******		−7.67	**<0.0001******
Age * age	3.37	**0.001*****		3.87	**0.002****
Gender	−0.86	0.390		−1.01	0.315
R occipital area	2.15	**0.034***	R parietal area	−1.07	0.286
R total cortical area	−2.85	**0.005****	R total cortical area	0.38	0.707

**** $p \leqslant 0.0001$.
*** $p \leqslant 0.001$.
** $p \leqslant 0.01$.
* $p \leqslant 0.05$.

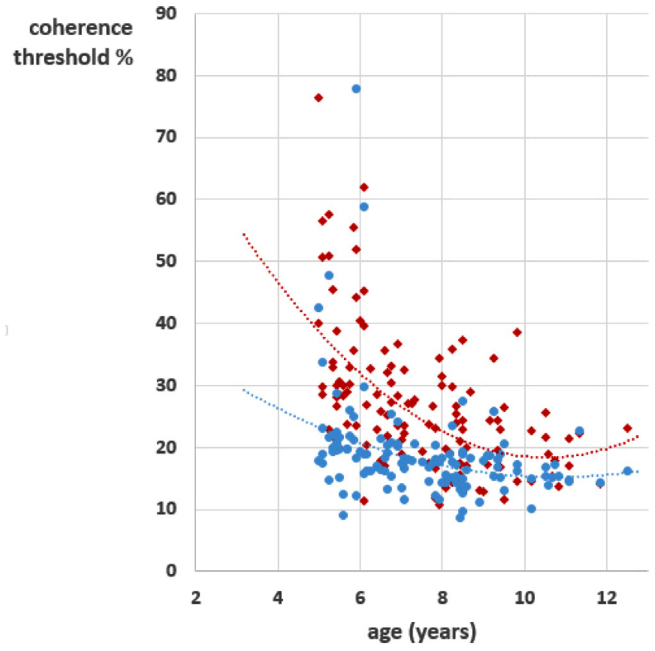

Fig. 3. Individual children's coherence thresholds for global motion (red diamonds) and global form (blue circles), plotted as a function of age. Each point is the mean of two measurements. The lines are quadratic fits to the data points. N = 125.

per improvement with age for global motion than for form, especially in the younger part of the range, and a greater individual variability for motion than for form. The approach to an asymptotic value around 8–9 years is consistent with these and other results (e.g. Braunitzer et al., 2012; see also review by Hadad et al., 2015). However, despite the different age functions, global form and motion thresholds had a substantial shared variance: when the effect of age was removed by analysing the studentized residuals for each threshold in a regression against age and gender, individual form and motion thresholds showed a correlation of $r = 0.597$.

3.2. Relation of coherence thresholds to fractional anisotropy in the superior longitudinal fasciculus

Table 2 summarises statistical models for the prediction of motion and form coherence thresholds from the fractional anisotropy measures of the superior longitudinal fasciculus. The right and left SLF were opposite predictors of global motion sensitivity: higher fractional anisotropy in the right-hemisphere's superior longitudinal fasciculus is associated with lower motion thresholds (high sensitivity), while higher fractional anisotropy in the left hemisphere's superior longitudinal fasciculus was associated with higher motion thresholds (low sensitivity). Fig. 4 shows leverage plots, (i.e. the unique effects of left and right fractional anisotropy respectively on global motion thresholds). In contrast to these results for global motion, no such relationship was found with global form sensitivity. Associations with global motion sensitivity but not global form were similarly found in the structural measures of cortical area reported by Braddick et al. (2016).

Similar models were tested for prediction by the whole skeleton fractional anisotropy. These yielded no significant associations with either global motion or global form sensitivity, either when entered alone into the model or alongside fractional anisotropy of right and left superior longitudinal fasciculus (Table 3). The latter result indicates that the associations with the left and right superior longitudinal fasciculus were anatomically specific and not a reflection of overall white matter maturation.

Since global motion performance was strongly associated with age in the range studied, one might ask whether the relationship with fractional anisotropy in the left and right superior longitudinal fasciculus reflects differential maturation between individual children, that is, was the asymmetry between the tracts a feature of the more mature brain? This appears unlikely. The average fractional anisotropy of the left and right increased with age ($t = 4.14$, $p < 0.0001$ in a model including age, age^2, and gender: see Fig. 5a). However an analogous model for the ratio (*left SLF FA*):(*right SLF FA*) showed no age effect and a very flat relation (Fig. 5b). Over the group as a whole, there was no significant difference between fractional anisotropy values for the left and right superior longitudinal fasciculi (means 0.497 and 0.499 respectively; matched-pairs $t = 1.206$, $p = 0.23$).

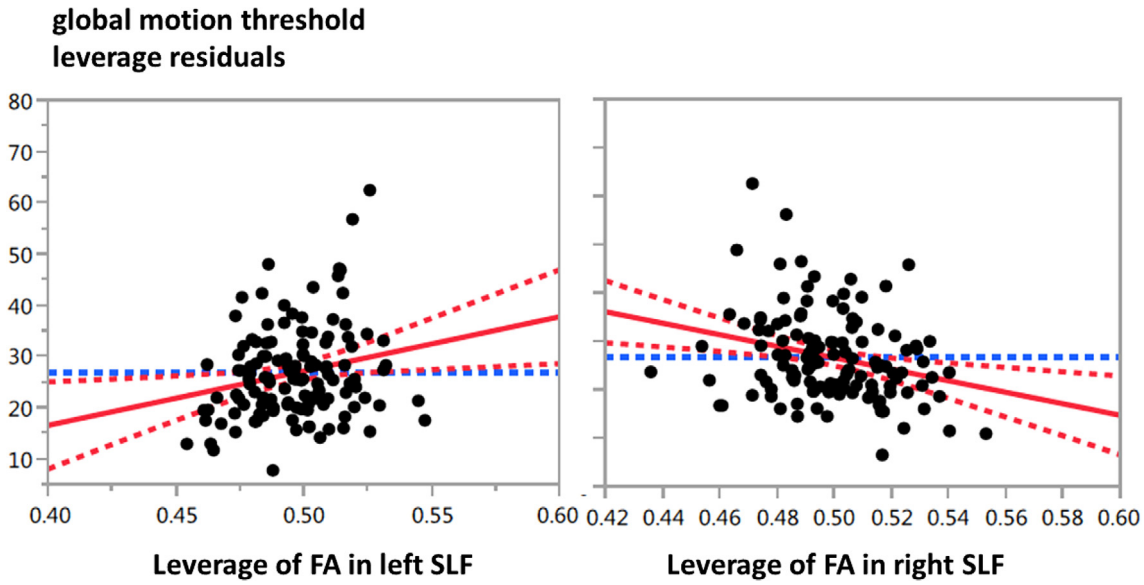

Fig. 4. Leverage plots of global motion thresholds against fractional anisotropy of the left and right superior longitudinal fasciculus. Leverage plots indicate the relationship between residuals when other variables in the model (age, age^2, and gender) are allowed for.

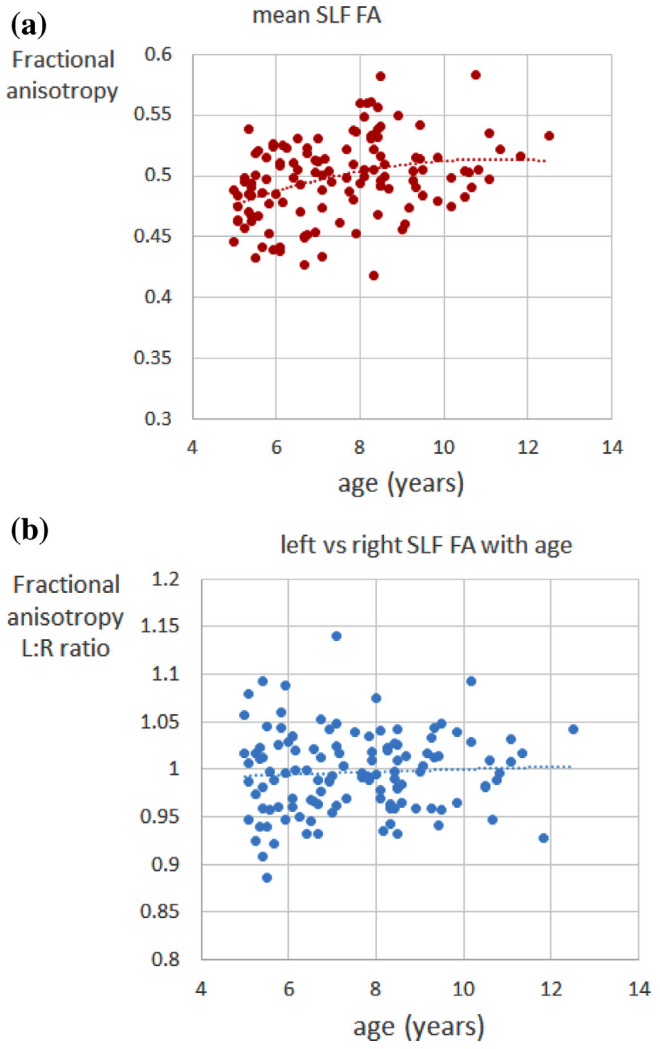

Fig. 5. (a) Scatter plot of mean fractional anisotropy of left and right superior longitudinal fasciculus for individual children, as a function of age. Dotted line is a quadratic fit (regression highly significant – see text); (b) scatter plot of the ratio of fractional anisotropy of left vs right superior longitudinal fasciculus for individual children, as a function of age. Dotted line is a quadratic fit (no significant age variation).

3.3. Associations with coherence thresholds in whole-brain fractional anisotropy data

The primary goal of this study was to test the specific anatomical hypotheses about the relationship between microstructure of white matter in the superior longitudinal fasciculus, and variations in children's sensitivity to global motion. Therefore neither a whole-brain, voxel-wise analysis of the effects (appropriately adjusted for multiple comparisons), nor a restricted voxel-wise analysis with small volume correction was considered appropriate for testing this *a priori* hypothesis. However, since the analyses we used produced estimates of the effect size at each voxel, we have provided visualization of the effect-size maps showing positive and negative associations between FA and motion coherence threshold, adjusted for age, age2, and gender (Fig. 6A–D). A similar effect size map for the positive and negative associations between FA and form coherence threshold is presented in Fig. 6E–G.

As well as the right superior longitudinal fasciculus, which was tested in our original hypothesis, clusters of voxels with negative association with motion coherence threshold were found in the corona radiata (Fig. 6C–D). The region in the right anterior corona radiata also overlaps strongly with voxels showing a negative association with form coherence thresholds (Fig. 6E, F). Finally, positive association with form coherence thresholds (i.e. high fractional anisotropy linked to low global form sensitivity) occurred in a midline region of the cerebellum (Fig. 6G). However, in no case did a voxel meet the criterion for significance at $p < 0.05$ when corrected for multiple comparisons. For the motion threshold, 1403 voxels had a t-value above 1.980 and 5183 voxels had a t-value below −1.980 (uncorrected $p < 0.05$), comprising 5.53% of the voxels in the skeleton. For the form threshold, 1811 voxels had a t-value above 1.980 and 3266 voxels had a t-value below −1.980 (uncorrected $p < 0.05$), comprising 4.27% of the voxels in the skeleton.

3.4. Superior longitudinal fasciculus and cortical area

The asymmetry in the relation between motion thresholds and left and right superior longitudinal fasciculus prompted us to re-examine the association of these thresholds with the area of cortical lobes. The analysis in Braddick et al. (2016) examined relationships with the total area of each lobe, combining left and right hemispheres. We have now tested regression models of these data in which left and right parietal and occipital lobes are examined separately. The results (Tables 4a and 4b) showed that the effects of area (lower motion thresholds with high parietal area, higher motion thresholds with high occipital area) were in the same direction for left and right hemispheres. However, the effects of parietal and occipital area previously reported in the bilateral data were driven most strongly by the areas of these lobes in the left hemisphere. Thus the overall results reflect a complex pattern of structural asymmetry, in which cortical area effects were dominated by the left hemisphere, where SLF fractional anisotropy shows a negative relation with motion performance, and the positive association of the right superior longitudinal fasciculus was accompanied by a weaker relationship of lobe areas to motion performance in that hemisphere.

Do these effects, nonetheless, reflect a common phenotype of asymmetrical brain development? This can be tested by a regression model which includes bilateral parietal area, together with fractional anisotropy in the right and the left superior longitudinal fasciculus (Table 5). Each of these structural measures made a significant, independent contribution to the prediction of global motion thresholds. These relationships, therefore, cannot depend primarily on shared variance between the structural measures. In fact, although fractional anisotropy of the left and right superior longitudinal fasciculi showed substantial shared variance, as did and left and right areas of parietal and occipital lobes, the correlations between fractional anisotropy of the superior longitudinal fasciculus and cortical area measures were very weak when age, overall area and whole skeleton fractional anisotropy are taken into account (Table 6).

4. Discussion

Our earlier analysis (Braddick et al., 2016) showed that children's global motion performance was related to variations in cortical structure in the parietal lobe, particularly in the region of the intraparietal sulcus (IPS). On this basis, we hypothesised that the superior longitudinal fasciculus, through which this area interacts with anterior cerebral structures, might show a similar relation to visual motion processing. Our results confirmed that such a link exists, but that it is complex, with opposite relationships between the structure of the superior longitudinal fasciculus and motion sensitivity in the two hemispheres. Furthermore, on closer examination, the relation with parietal and occipital cortical areas also was found to be asymmetrical. The sign was the same in both

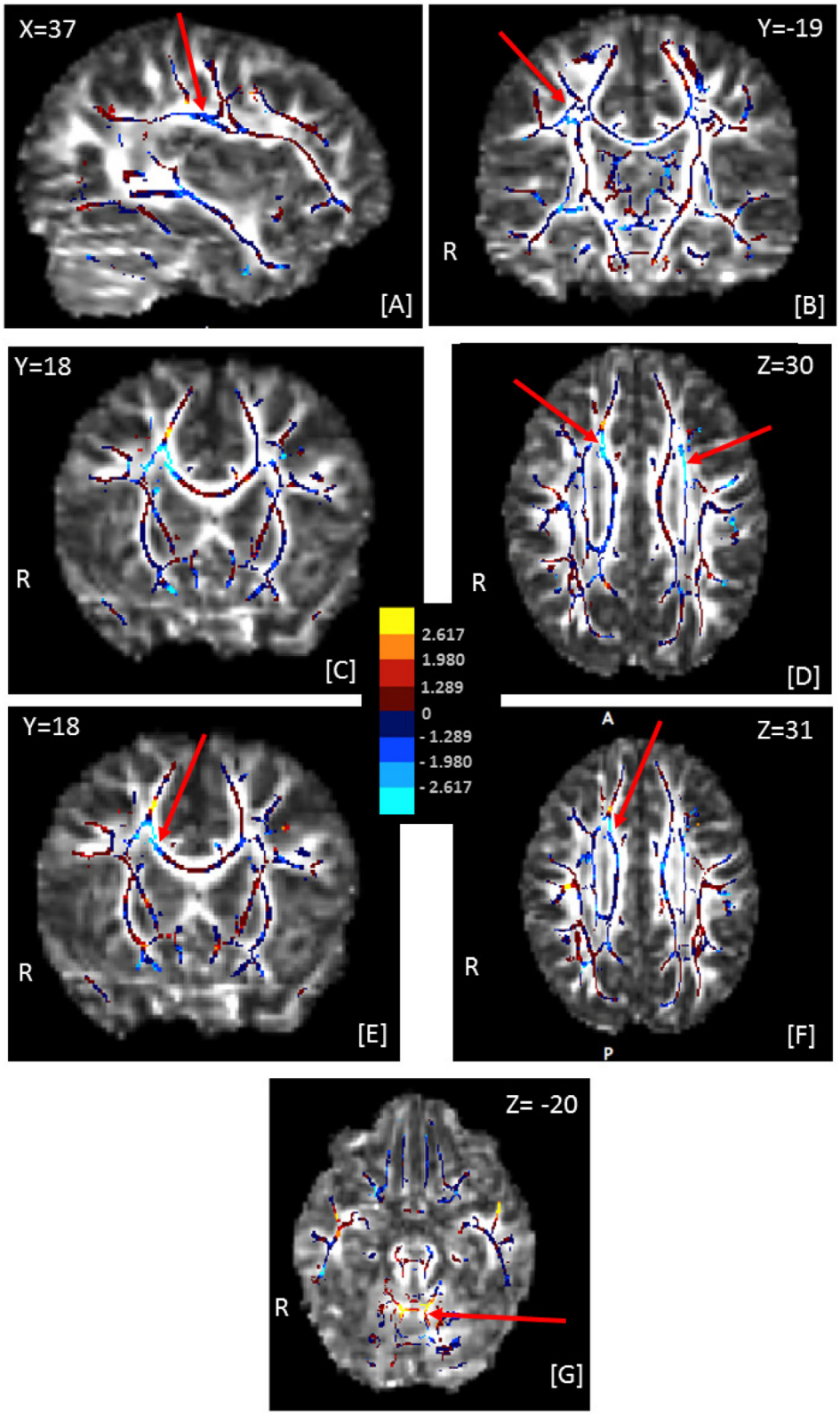

Fig. 6. Effect-size maps of the associations between global thresholds and fractional anisotropy (FA), adjusted for age, age^2, and gender. The effect-size maps are overlaid on the target FA image. The center panel shows the mapping of colors to values of the t-statistics. All voxels on the skeleton are colored. $|t| > 1.980$ corresponds to an uncorrected p value of <0.05, and $|t| > 2.617$ to $p < 0.01$. The MNI coordinates for each section are indicated on the image, along with R indicating the right hemisphere and A, P the anterior-posterior orientation of the axial section [F]. Red arrows indicate clusters of voxels discussed in Section 3.3. Negative associations mean that high FA was associated with high sensitivity (low threshold). [A]–[D] Show effect sizes for the correlation of global *motion* thresholds with FA: [A], [B]: cluster of voxels in the right superior longitudinal fasciculus showing a negative association with motion coherence threshold; [C], [D]: clusters of voxels in right anterior and left superior corona radiata, showing a negative association with motion coherence thresholds. [E]–[G] Show effect sizes for the correlation of global *form* thresholds with FA: [E], [F]: cluster of voxels in right anterior corona radiata showing a negative association with form coherence thresholds; [G] cluster of voxels in the cerebellum showing a positive association with form coherence thresholds. (For interpretation of the references to color in this figure legend, the reader is referred to the web version of this article.)

Table 6
Matrix of intercorrelations between structural measures. All measures residualised for age and gender. Area measures are also residualised for total cortical area; FA measures are residualised for whole skeleton FA. Significance levels, where not stated, are all p > 0.05.

	R parietal area	L occipital area	R occipital area	L SLF FA	R SLF FA
L parietal area	0.356 *P < 0.001*	−0.408 *p < 0.001*	−0.400 *p < 0.001*	−0.111	−0.031
R parietal area		−0.240 *p < 0.01*	−0.268 *p < 0.01*	−0.173 *p = 0.532*	−0.045
L occipital area			0.783 *p < 0.001*	0.173 *p = 0.539*	0.097
R occipital area				0.090	−0.034
L SLF FA					0.698 *p < 0.001*

hemispheres, but was markedly stronger for the left hemisphere. Thus the brain of the child who has high sensitivity to global motion shows a complex pattern of asymmetry relative to the brain of a child with lower performance, although the different components of this asymmetry contribute independently, at least to some degree.

Csete et al. (2014) have also reported a relationship between motion coherence threshold and fractional anisotropy for some voxels in a number of white matter regions, in a smaller group of adult participants. They did not test specific tracts, although they state that some of the locations they identify lie within the medial branch of the left superior longitudinal fasciculus. For all the voxels they reported, the correlation of fractional anisotropy with motion thresholds is positive – that is, higher fractional anisotropy goes with reduced sensitivity, in line with our own finding for the left SLF.

We tested a specific hypothesis of association between global visual performance and the superior longitudinal fasciculus. The whole-skeleton analysis of effect size allows us to examine how this association may be distributed in white matter. Additional locations for association were found in the corona radiata. These included a region of the right anterior corona radiata which was associated with both global motion and global form sensitivity, and so may play a different role to the apparently motion-specific structure in the superior longitudinal fasciculus. While the corona radiata is most often thought of as the fan of fibres which converge into the internal capsule and project to subcortical and spinal targets, it does include cortico-cortical tracts also (Wakana, Jiang, Nagae-Poetscher, van Zijl, & Mori, 2004). Fractional anisotropy in the corona radiata has been associated with individual variations in a number of cognitive functions, including children's numerical abilities (Matejko & Ansari, 2015), cognitive control (Chaddock-Heyman et al., 2013; Seghete, Herting, & Nagel, 2013; literacy (Myers et al., 2014), and IQ scores (Chiang et al., 2009). This structure may therefore be associated rather broadly with the development of information processing abilities, and its specific role in brain networks subserving these abilities, and in global visual processes specifically, is unclear. In any case, given that this and other relationships shown in the effect size maps have only been shown with uncorrected significance levels, they must be seen as pointers for possible further investigation rather than established findings.

4.1. Asymmetries in motion processing

A number of reports find that individual participants show hemispheric asymmetries in cerebral responses to motion, for example, Patzwahl, Zanker, and Altenmuller (1994), Hollants-Gilhuijs, De Munck, Kubova, van Royen, and Spekreijse (2000), and Nakamura et al. (2003), which they ascribe to area V5/MT. However, there does not appear to be any consistent difference across individuals between left and right hemispheres in these responses, which might be associated with the asymmetric anatomical relationships we find with motion coherence thresholds. An exception is an overall right-hemisphere advantage reported by Patzwahl et al. (1994), which is ascribed by them to "[the special role of the right hemisphere] attentional system amplifying the activation of the right parietal cortex". In contrast, Hollants-Gilhuijs, Ruijter, and Spekreijse (1998) found a behavioral advantage for right-field motion detection (implying left-hemisphere advantage) in 6- to 16-year-old children (but not in adults), which they ascribed to differential maturation of extra-striate areas in the two hemispheres. A number of other visuo-spatial tasks have been found to show hemispheric asymmetries, not necessarily in this direction (e.g. Atkinson & Egeth, 1973). Since our task involved intermixed left- and right-field stimuli, and the children could freely fixate while making their decision, our data provide no evidence on half-field differences and do not allow us to examine whether such a functional asymmetry is linked to the structural correlates we find. This is a possible question for future studies using a task which requires central fixation and brief stimulus presentations in either left or right field, which would not however be practical with children across the age range of the present study.

4.2. Attentional and cognitive role of the superior longitudinal fasciculus

Our findings present a specific link of structure of the superior longitudinal fasciculus to the processing of motion information. However, neuroimaging and lesion studies in adults have identified a number of broader aspects of cognitive function that are associated with this tract, especially within the domain of spatial cognition and attention. Bennett, Motes, Rao, and Rypma (2012), Mayer and Vuong (2014) and Chechlacz, Gillebert, Vangkilde, Petersen, and Humphreys (2015) report correlations of fractional anisotropy in the superior longitudinal fasciculus with various measures of visuo-spatial attention; Rodríguez-Herreros et al. (2015) find that fractional anisotropy in SLF-2 correlates with the individual resistance to TMS disruption in visually guided reaching. Damage to the superior longitudinal fasciculus is also a key cause of the spatial neglect syndrome (e.g. Chechlacz, Rotshtein, & Humphreys, 2012; Lunven & Bartolomeo, 2016; Ptak & Schnider, 2010; Shinoura et al., 2009). A number of studies show associations between the SLF and numerical cognition (Matejko & Ansari, 2015), consistent with our finding that these are linked to motion sensitivity (Braddick et al., 2016).

Other associations have been found between fractional anisotropy of the superior longitudinal fasciculus, and working memory (Rizio & Diaz, 2016; Vestergaard et al., 2011), executive function and sustained attention in children (Klarborg et al., 2013; Urger et al., 2015), and children's reading development (Travis, Ben-Shachar, Myall, & Feldman, 2016; Wang et al., 2016).

Fractional anisotropy in the superior longitudinal fasciculus is also reduced compared to controls in several neurodevelopmental disorders, including cerebral palsy, where it is correlated with IQ (Ballester-Plané et al., 2016) and amblyopia, where it is correlated with visual acuity (Li et al., 2015). It is also correlated with response time variability in attention-deficit hyperactivity disorder (Wolfers et al., 2015). However in Williams Syndrome, fractional anisotropy of the superior longitudinal fasciculus is increased relative to controls, and high fractional anisotropy is associated with poor visuospatial performance (Hoeft et al., 2007).

More broadly, early disorders of cerebral white matter are a major feature of neonatal brain injury associated with deficits of early attention and dorsal stream function in preterm born children (Atkinosn & Braddick, 2007; Atkinson et al., 2008) and of early brain development in Williams syndrome (Mercuri et al., 1997).

The networks associated with spatial attention are not symmetrical: Thiebaut de Schotten et al. (2011) describe a "lateralized brain network for visuospatial attention" in which the volume of right SLF II is associated with left bias in line bisection and with faster left field detection. These results, and the wider findings of attention-related functions suggest that our finding of fractional anisotropy of the right superior longitudinal fasciculus associated with good motion performance may be linked to deployment of attention in the motion processing task. Studies of functional connectivity (Friston & Büchel, 2000) have shown that activity in the parietal lobe is associated with attentional modulation of the transmission of motion information from V1/V2-V5/MT. However, it should be noted that the global form task, which shares many of the attention demands of the global motion task, shows none of the same relations with brain structure.

The relationship between fractional anisotropy and function is complex, since a number of different tissue properties will contribute to the measured FA (Beaulieu, 2002). It is often assumed that fractional anisotropy reflects the integrity of tract organization, in terms of the parallelism and packing of axons which restricts radial diffusion and hence increases fractional anisotropy; myelination is another functionally important aspect of brain development which similarly increases fractional anisotropy. However, some factors which reduce fractional anisotropy may be associated with enhanced function: for example increased axonal diameter which may be responsible for the association seen between faster choice reaction time and reduced fractional anisotropy in the optic radiation (Tuch et al., 2005). Hoeft et al. (2007), discussing the increased fractional anisotropy and its association with poor visuospatial test performance in Williams Syndrome, suggest that this higher fractional anisotropy may be associated with reduced branching in the tract, a proposed characteristic of this neurodevelopmental disorder (Eckert et al., 2006). Thus we cannot necessarily assume that a positive correlation with high fractional anisotropy means that a particular fibre tract contributes positively to motion processing in development (or vice versa for a negative correlation). Furthermore, the direction of causality between behavioral performance and structural differences remains uncertain.

5. Conclusions

The finding that the structure of the superior longitudinal fasciculus is related to individual variations in children's global motion processing adds support to two conclusions from our earlier findings on their relation to regional cortical area (Braddick et al., 2016).

First, these individual differences do not necessarily reflect the stage, in extrastriate areas such as MT/V5 or V3a, where local motion signals are initially integrated to provide information about globally coherent motion (Braddick et al., 2001; Mikami, Newsome, & Wurtz, 1986; Newsome & Paré, 1988), although we cannot exclude localized variations in these areas. Instead, the correlations with individual differences in global motion sensitivity are provided by variations in the area of the parietal lobe (which receives input from extrastriate motion areas), and in the superior longitudinal fasciculus through which parietal cortex communicates with anterior cerebral areas. These results suggest that the critical point for determining these individual differences may be the levels where sensory evidence for global motion is accumulated for perceptual decision-making, and at which these decisions are communicated to response systems (Hanks, Ditterich, & Shadlen, 2006; Shadlen & Newsome, 2001). The role of attention systems in contributing to this performance has been discussed above; top-down modulation of parietal function may play an important role in individual differences.

Second, we identify structural correlates of global motion sensitivity but have not yet confirmed any for sensitivity to static global form. Impaired motion rather than form sensitivity provides the widespread signature of neurodevelopmental disorders ("dorsal stream vulnerability" – Braddick et al., 2003). It appears that even within the range of typical development, it is again motion processing which provides the more sensitive index of variations in brain development.

The developmental course of these structure-function relationships is still unknown. Future work using longitudinal data sets from this and other groups of children may help to show whether early structural differences predict later functional development. Studies of genetic associations with motion thresholds and with brain structure (e.g. Schork et al., 2012) may also help to understand the causal pathways that determine these patterns of individual differences.

Acknowledgments

This work was supported by the National Institute on Drug Abuse of the National Institutes of Health and by the *Eunice Kennedy Shriver* National Institute of Child Health & Human Development of the National Institutes of Health (grant numbers RC2DA029475, R01HD061414, R24HD075489). JA received support from an Emeritus Fellowship from the Leverhulme Foundation. We thank the members of the PLING Data Camp team for assistance with data collection, and the participating children and their families.

References

Akshoomoff, N., Newman, E., Thompson, W. K., McCabe, C., Bloss, C. S., Chang, L., ... Jernigan, T. L. (2014). The NIH Toolbox Cognition Battery: Results from a large normative developmental sample (PING). *Neuropsychology, 28*, 1–10.

Andersson, J. L. R., Jenkinson, M., & Smith, S. (2007). Non-linear optimisation. FMRIB Technical Report TR07JA1 from <www.fmrib.ox.ac.uk/analysis/techrep>.

Andersson, J. L. R., Jenkinson, M., & Smith, S. (2007). Non-linear registration, aka Spatial normalisation. FMRIB technical report TR07JA2 from <www.fmrib.ox.ac.uk/analysis/techrep>.

Atkinson, J. (in press). The Davida Teller Award Lecture, 2016. Visual Brain Development: a review of 'Dorsal Stream vulnerability' – motion, mathematics, amblyopia, actions and attention. Journal of Vision.

Atkinson, J., & Braddick, O. (2005). Dorsal stream vulnerability and autistic disorders: The importance of comparative studies of form and motion coherence in typically developing children and children with developmental disorders. *Cahiers de Psychologie Cognitive (Current Psychology of Cognition), 23* (1–2), 49–58.

Atkinson, J., & Braddick, O. J. (2007). Visual and visuocognitive development in children born very prematurely. *Progress in Brain Research, 164*, 123–149.

Atkinson, J., & Braddick, O. (2011). From genes to brain development to phenotypic behavior: "Dorsal-stream vulnerability" in relation to spatial cognition, attention, and planning of actions in Williams syndrome (WS) and other developmental disorders. *Progress in Brain Research, 189*, 261–283.

Atkinson, J., Braddick, O., Anker, S., Curran, W., & Andrew, R. (2003). Neurobiological models of visuospatial cognition in children with Williams Syndrome:

Measures of dorsal-stream and frontal function. *Developmental Neuropsychology, 23*, 141–174.
Atkinson, J., Braddick, O., Anker, S., Nardini, M., Birtles, D., Rutherford, M., ... Cowan, F. (2008). Cortical vision, MRI and developmental outcome in preterm infants. *Archives of Disease in Childhood, 93*, F292–F297.
Atkinson, J., Braddick, O., Rose, F. E., Searcy, Y. M., Wattam-Bell, J., & Bellugi, U. (2006). Dorsal-stream motion processing deficits persist into adulthood in Williams Syndrome. *Neuropsychologia, 44*, 828–833.
Atkinson, J., Braddick, O., Wattam-Bell, J., Akshoomoff, N., Newman, E., Girard, H., ... Jernigan, T. (2014). Global motion, mathematics and movement: Dorsal stream sensitivity relates to children's individual differences in cognitive abilities and regional brain development. [Abstract]. *Journal of Vision, 14*(10). 1324-1324.
Atkinson, J., & Egeth, H. (1973). Right hemisphere superiority in visual orientation matching. *Canadian Journal of Psychology, 27*, 152–158.
Atkinson, J., King, J., Braddick, O., Nokes, L., Anker, S., & Braddick, F. (1997). A specific deficit of dorsal stream function in Williams' syndrome. *NeuroReport, 8*, 1919–1922.
Ballester-Plané, J., Laporta-Hoyos, O., Macaya, A., Póo, P., Meléndez-Plumed, M., Vázquez, É., ... Pueyo, R. (2016). Measuring intellectual ability in cerebral palsy: The comparison of three tests and their neuroimaging correlates. *Research in Developmental Disabilities, 56*, 83–98.
Beaulieu, C. (2002). The basis of anisotropic water diffusion in the nervous system—A technical review. *NMR in Biomedicine, 15*, 435–455.
Bennett, I. J., Motes, M. A., Rao, N. K., & Rypma, B. (2012). White matter tract integrity predicts visual search performance in young and older adults. *Neurobiology of Aging, 33*(433), e21–e31.
Braddick, O., & Atkinson, J. (2011). Development of human visual function. *Vision Research, 51*, 1588–1609.
Braddick, O., Atkinson, J., Newman, E., Akshoomoff, N., Kuperman, J. M., Bartsch, H., ... Jernigan, T. L. (2016). Global visual motion sensitivity: Associations with parietal area and children's mathematical cognition. *Journal of Cognitive Neuroscience, 2016*(26), 1–12. Epub ahead of print.
Braddick, O., Atkinson, J., & Wattam-Bell, J. (2003). Normal and anomalous development of visual motion processing: Motion coherence and 'dorsal stream vulnerability'. *Neuropsychologia, 41*, 1769–1784.
Braddick, O. J., O'Brien, J. M. D., Wattam-Bell, J., Atkinson, J., Hartley, T., & Turner, R. (2001). Brain areas sensitive to coherent visual motion. *Perception, 30*, 61–72.
Braunitzer, G., Rokszin, A., Kóbor, J., Benedek, G., Nagy, A., & Kincses, T. Z. (2012). Delayed development of visual motion processing in childhood migraine. *Cephalalgia, 32*, 492–496.
Brown, T. T. (2016), Individual differences in human brain development. WIREs Cognitive Science. doi:http://dx.doi.org/10.1002/wcs.1389.
Brown, T. T., Kuperman, J. M., Chung, Y., Erhart, M., McCabe, C., Hagler, D. J., ... Dale, A. M. (2012). Neuroanatomical assessment of biological maturity. *Current Biology, 22*, 1693–1698.
Chaddock-Heyman, L., Erickson, K. I., Voss, M. W., Powers, J. P., Knecht, A. M., Pontifex, M. B., ... Kramer, A. F. (2013). White matter microstructure is associated with cognitive control in children. *Biological Psychology, 94*, 109–115.
Chechlacz, M., Gillebert, C. R., Vangkilde, S. A., Petersen, A., & Humphreys, G. W. (2015). Structural variability within frontoparietal networks and individual differences in attentional functions: An approach using the theory of visual attention. *Journal of Neuroscience, 35*, 10647–10658.
Chechlacz, M., Rotshtein, P., & Humphreys, G. W. (2012). Neuroanatomical dissections of unilateral visual neglect symptoms: ALE meta-analysis of lesion-symptom mapping. *Frontiers in Human Neuroscience*. http://dx.doi.org/10.3389/fnhum.2012.00230.
Chen, C.-H., Gutierrez, E. D., Thompson, W., Panizzon, M. S., Jernigan, T. L., Eyler, L. T., ... Dale, A. M. (2012). Hierarchical genetic organization of human cortical surface area. *Science, 335*, 1634–1636.
Chiang, M. C., Barysheva, M., Shattuck, D. W., Lee, A. D., Madsen, S. K., Avedissian, C., ... Thompson, P. M. (2009). Genetics of brain fiber architecture and intellectual performance. *Journal of Neuroscience, 29*, 2212–2224.
Csete, G., Szabo, N., Rokszin, A., Toth, E., Braunitzer, G., Benedek, G., ... Tamas Kincses, Z. (2014). An investigation of the white matter microstructure in motion detection using diffusion MRI. *Brain Research, 1570*, 35–42.
Eckert, M. A., Galaburda, A. M., Mills, D. L., Bellugi, U., Korenberg, J. R., & Reiss, A. L. (2006). The neurobiology of Williams syndrome: Cascading influences of visual system impairment? *Cellular & Molecular Life Sciences, 63*, 1867–1875.
Ellemberg, D., Lewis, T. L., Maurer, D., Brar, S., & Brent, H. P. (2002). Better perception of global motion after monocular than after binocular deprivation. *Vision Research, 42*, 169–179.
Fjell, A. M., Walhovd, K. B., Brown, T. T., Kuperman, J. M., Chung, Y., & Hagler, D. J. Jr., ... For the Pediatric Imaging, Neurocognition, and Genetics Study. (2012). Multimodal imaging of the self-regulating developing brain. *Proceedings of the National Academy of Sciences of the United States of America, 109*, 19620–19625.
Fjell, A. M., Westlye, L. T., Amlien, I., Tamnes, C. K., Grydeland, H., Engvig, A., ... Walhovd, K. B. (2015). High-expanding cortical regions in human development and evolution are related to higher intellectual abilities. *Cerebral Cortex, 25*, 26–34.
Friston, K. J., & Büchel, C. (2000). Attentional modulation of effective connectivity from V2 to V5/MT in humans. *Proceedings of the National Academy of Sciences of the United States of America, 97*, 7591–7596.
Goodbourn, P. T., Bosten, J. M., Hogg, R. E., Bargary, G., Lawrance-Owen, A. J., & Mollon, J. D. (2012). Do different 'magnocellular tasks' probe the same neural substrate? *Proceedings of the Royal Society B, 279*, 4263–4271.
Gunn, A., Cory, E., Atkinson, J., Braddick, O., Wattam-Bell, J., Guzzetta, A., & Cioni, G. (2002). Dorsal and ventral stream sensitivity in normal development and hemiplegia. *NeuroReport, 13*, 843–847.
Hadad, B. S., Maurer, D., & Lewis, T. L. (2011). Long trajectory for the development of sensitivity to global and biological motion. *Developmental Science, 14*, 1330–1339.
Hadad, B. S., Schwartz, S., Maurer, D., & Lewis, T. L. (2015). Motion perception: a review of developmental changes and the role of early visual experience. *Frontiers in Integrative Neuroscience, 9*, 49.
Hanks, T. D., Ditterich, J., & Shadlen, M. N. (2006). Microstimulation of macaque area LIP affects decision-making in a motion discrimination task. *Nature Neuroscience, 9*, 682–689.
Hansen, P. C., Stein, J. F., Orde, S. R., Winter, J. L., & Talcott, J. B. (2001). Are dyslexics' visual deficits limited to measures of dorsal stream function? *NeuroReport, 12*, 1527–1530.
Ho, C. S., Giaschi, D. E., Boden, C., Dougherty, R., Cline, R., & Lyons, C. (2005). Deficient motion perception in the fellow eye of amblyopic children. *Vision Research, 45*, 1615–1627.
Hoeft, F., Barnea-Goraly, N., Haas, B. W., Golarai, G., Ng, D., Mills, D., ... Reiss, A. L. (2007). More is not always better: Increased fractional anisotropy of superior longitudinal fasciculus associated with poor visuospatial abilities in Williams syndrome. *Journal of Neuroscience, 27*, 11960–11965.
Hollants-Gilhuijs, M. A. M., De Munck, J. C., Kubova, Z., van Royen, E., & Spekreijse, H. (2000). The development of hemispheric asymmetry in human motion VEPs. *Vision Research, 40*, 1–11.
Hollants-Gilhuijs, M. A. M., Ruijter, J. M., & Spekreijse, H. (1998). Visual half-field development in children: Detection of motion-defined forms. *Vision Research, 38*, 651–657.
Jernigan, T. L., Brown, T. T., Hagler, D. J., Jr., Akshoomoff, N., Bartsch, H., & Newman, E. ... Pediatric Imaging, Neurocognition and Genetics Study. (2016). The Pediatric Imaging, Neurocognition, and Genetics (PING) data repository. *Neuroimage, 124*(Pt. B), 1149–1154.
Kamali, A., Flanders, A. E., Brody, J., Hunter, J. V., & Hasan, K. M. (2014). Tracing superior longitudinal fasciculus connectivity in the human brain using high resolution diffusion tensor tractography. *Brain Structure & Function, 219*, 269–281.
Klarborg, B., Skak Madsen, K., Vestergaard, M., Skimminge, A., Jernigan, T. L., & Baaré, W. F. (2013). Sustained attention is associated with right superior longitudinal fasciculus and superior parietal white matter microstructure in children. *Human Brain Mapping, 34*, 3216–3232.
Kogan, C. S., Boutet, I., Cornish, K., Zangenehpour, S., Mullen, K. T., Holden, J. J. A., ... Chaudhuri, A. (2004). Differential impact of the FMR1 gene on visual processing in fragile X syndrome. *Brain, 127*, 591–601.
Kontsevich, L. L., & Tyler, C. W. (1999). Bayesian adaptive estimation of psychometric slope and threshold. *Vision Research, 39*, 2729–2737.
Kravitz, D. J., Saleem, K. S., Baker, C. I., & Mishkin, M. (2011). A new neural framework for visuospatial processing. *Nature Reviews Neuroscience, 12*, 217–230.
Lewis, T. L., Ellemberg, D., Maurer, D., Wilkinson, F., Wilson, H. R., Dirks, M., & Brent, H. P. (2002). Sensitivity to global form in Glass patterns after early visual deprivation in humans. *Vision Research, 42*, 939–948.
Li, Q., Zhai, L., Jiang, Q., Qin, W., Li, Q., Yin, X., & Guo, M. (2015). Tract-based spatial statistics analysis of white matter changes in children with anisometropic amblyopia. *Neuroscience Letters, 597*, 7–12.
Lunven, M., & Bartolomeo, P. (2016). Attention and spatial cognition: Neural and anatomical substrates of visual neglect. *Annals of Physical & Rehabilitation Medicine*. http://dx.doi.org/10.1016/j.rehab.2016.01.004. Epub ahead of print.
Makris, N., Kennedy, D. N., McInerney, S., Sorensen, A. G., Wang, R., Caviness, V. S., Jr., & Pandya, D. N. (2005). Segmentation of subcomponents within the superior longitudinal fascicle in humans: A quantitative, in vivo, DT-MRI study. *Cerebral Cortex, 15*, 854–869.
Matejko, A. A., & Ansari, D. (2015). Drawing connections between white matter and numerical and mathematical cognition: A literature review. *Neuroscience and Biobehavioral Reviews, 48*(2015), 35–52.
Mayer, K. M., & Vuong, Q. C. (2014). TBSS and probabilistic tractography reveal white matter connections for attention to object features. *Brain Structure & Function, 219*, 2159–2171.
Meier, K., & Giaschi, D. (2014). The maturation of global motion perception depends on the spatial and temporal offsets of the stimulus. *Vision Research, 95*, 61–67.
Mercuri, E., Atkinson, J., Braddick, O., Rutherford, M., Cowan, F., Counsell, S., ... Bydder, G. (1997). Chiari I malformation and white matter changes in asymptomatic young children with Williams syndrome: Clinical and MRI study. *European Journal of Pediatric Neurology, 5/6*, 177–181.
Mesulam, M. M. (1981). A cortical network for directed attention and unilateral neglect. *Annals of Neurology, 10*, 309–325.
Mikami, A., Newsome, W. T., & Wurtz, R. H. (1986). Motion selectivity in macaque visual cortex. I. Mechanisms of direction and speed selectivity in extrastriate area MT. *Journal of Neurophysiology, 55*, 1308–1327.
Mori, S., Wakana, S., Nagae-Poetscher, L. M., & van Zijl, P. C. (2005). *MRI atlas of human white matter*. Amsterdam: Elsevier.
Myers, C. A., Vandermosten, M., Farris, E. A., Hancock, R., Gimenez, P., Black, J. M., ... Hoeft, F. (2014). White matter morphometric changes uniquely predict children's reading acquisition. *Psychological Science, 25*, 1870–1883.
Nakamura, H., Kashii, S., Nagamine, T., Matsui, Y., Hashimoto, T., Honda, Y., & Shibasaki, H. (2003). Human V5 demonstrated by magnetoencephalography

using random dot kinematograms of different coherence levels. *Neuroscience Research, 46*, 423–433.

Newman, E., Thompson, W. K., Bartsch, H., Hagler, D. J., Jr, Chen, C. H., Brown, T. T., ... Jernigan, T. L. (2016). Anxiety is related to indices of cortical maturation in typically developing children and adolescents. *Brain Structure & Function, 221*, 3013–3025. http://dx.doi.org/10.1007/s00429-015-1085-9. Epub ahead of print.

Newsome, W. T., & Paré, E. B. (1988). A selective impairment of motion perception following lesions of the middle temporal visual area (MT). *Journal of Neuroscience, 8*, 2201–2211.

Patzwahl, D. R., Zanker, J. M., & Altenmuller, E. O. (1994). Cortical potentials reflecting motion processing in humans. *Visual Neuroscience, 11*, 1135–1147.

Peterzell, D. H. (2016). Discovering sensory processes using individual differences: A review and factor analytic manifesto. In: *Proceedings of the 2016 IS&T Symposium on Electronic Imaging: Conference on Human Vision and Electronic Imaging*.

Ptak, R., & Schnider, A. (2010). The dorsal attention network mediates orienting toward behaviorally relevant stimuli in spatial neglect. *Journal of Neuroscience, 30*, 12557–12565.

Rizio, A. A., & Diaz, M. T. (2016). Language, aging, and cognition: Frontal aslant tract and superior longitudinal fasciculus contribute toward working memory performance in older adults. *NeuroReport, 27*, 689–693.

Rodríguez-Herreros, B., Amengual, J. L., Gurtubay-Antolín, A., Richter, L., Jauer, P., Erdmann, C., ... Münte, T. F. (2015). Microstructure of the superior longitudinal fasciculus predicts stimulation-induced interference with on-line motor control. *Neuroimage, 120*, 254–265.

Schork, A. J., Madsen, K. S., Baare, W. F. C., Akshoomoff, N., McCabe, C., Erik Newman, E., et al. (2012). Common repeat polymorphism in the dopamine transporter gene SLC6A3 is associated with stop signal reaction time (SSRT) and motion coherence threshold (MCT). Presentation 393.13 at the 2012 Annual Meeting of the Society for Neuroscience, New Orleans, LA. <http://www.abstractsonline.com/Plan/ViewAbstract.aspx?sKey=0bb2fe49-2960-4a09-994f-0dfaa250eecc&cKey=8afe990a-c63c-467f-b881-3c63b4d843a0&mKey=%7b70007181-01C9-4DE9-A0A2-EEBFA14CD9F1%7d>.

Seghete, K. L., Herting, M. M., & Nagel, B. J. (2013). White matter microstructure correlates of inhibition and task-switching in adolescents. *Brain Research, 1527*, 15–28.

Shadlen, M. N., & Newsome, W. T. (2001). Neural basis of a perceptual decision in the parietal cortex (area LIP.) of the rhesus monkey. *Journal of Neurophysiology, 86*, 1916–1936.

Shinoura, N., Suzuki, Y., Yamada, R., Tabei, Y., Saito, K., & Yagi, K. (2009). Damage to the right superior longitudinal fasciculus in the inferior parietal lobe plays a role in spatial neglect. *Neuropsychologia, 47*, 2600–2603.

Simmers, A., Ledgeway, T., & Hess, R. (2005). The influences of visibility and anomalous integration processes on the perception of global spatial form versus motion in human amblyopia. *Vision Research, 45*, 449–460.

Simmons, D. R., Robertson, A. E., McKay, L. S., Toal, E., McAleer, P., & Pollick, F. E. (2009). Vision in autism spectrum disorders. *Vision Research, 49*, 2705–2739.

Smith, S. M., Jenkinson, M., Johansen-Berg, H., Rueckert, D., Nichols, T. E., Mackay, C. E., ... Behrens, T. E. (2006). Tract-based spatial statistics: Voxelwise analysis of multi-subject diffusion data. *Neuroimage, 31*, 1487–1505.

Smith, S. M., Jenkinson, M., Woolrich, M. W., Beckmann, C. F., Behrens, T. E. J., Johansen-Berg, H., ... Matthews, P. M. (2004). Advances in functional and structural MR image analysis and implementation as FSL. *NeuroImage, 23*(S1), 208–219.

Spencer, J., O'Brien, J., Riggs, K., Braddick, O., Atkinson, J., & Wattam-Bell, J. (2000). Motion processing in autism: Evidence for a dorsal stream deficiency. *NeuroReport, 11*, 2765–2767.

Szczepanski, S. M., Konen, C. S., & Kastner, S. (2010). Mechanisms of spatial attention control in frontal and parietal cortex. *Journal of Neuroscience, 30*, 148–160.

Taylor, N. M., Jakobson, L. S., Maurer, D., & Lewis, T. L. (2009). Differential vulnerability of global motion, global form, and biological motion processing in full-term and preterm children. *Neuropsychologia, 47*, 2766–2778.

Thiebaut de Schotten, M., Dell'Acqua, F., Forkel, S. J., Simmons, A., Vergani, F., Murphy, D. G., & Catani, M. (2011). A lateralized brain network for visuospatial attention. *Nature Neuroscience, 14*, 1245–1246.

Travis, K. E., Ben-Shachar, M., Myall, N. J., & Feldman, H. M. (2016). Variations in the neurobiology of reading in children and adolescents born full term and preterm. *Neuroimage: Clinical, 11*, 555–565.

Tuch, D. S., Salat, D. H., Wisco, J. J., Zaleta, A. K., Hevelone, N. D., & Rosas, H. D. (2005). Choice reaction time performance correlates with diffusion anisotropy in white matter pathways supporting visuospatial attention. *Proceedings of the National Academy of Sciences of the United States of America, 102*, 12212–12217.

Urger, S. E., De Bellis, M. D. S. R., Donald, P., Woolley, P. D., Chen, S. D., & Provenzale, J. (2015). The superior longitudinal fasciculus in typically developing children and adolescents: Diffusion Tensor Imaging and neuropsychological correlates. *Journal of Child Neurology, 30*, 9–20.

Vestergaard, M., Madsen, K. S., Baaré, W. F., Skimminge, A., Ejersbo, L. R., Ramsøy, T. Z., ... Jernigan, T. L. (2011). White matter microstructure in superior longitudinal fasciculus associated with spatial working memory performance in children. *Journal of Cognitive Neuroscience, 23*, 2135–2146.

Wakana, S., Jiang, H., Nagae-Poetscher, L. M., van Zijl, P. C. M., & Mori, S. (2004). Fiber tract-based atlas of human white matter anatomy. *Radiology, 230*, 77–87.

Wang, Y., Mauer, M. V., Raney, T., Peysakhovich, B., Becker, B. L., Sliva, D. D., & Gaab, N. (2016). Development of tract-specific white matter pathways during early reading development in at-risk children and typical controls. *Cerebral Cortex*. Epub ahead of print.

Wolfers, T., Onnink, A. M. H., Zwiers, M. P., Arias-Vasquez, A., Hoogman, M., Mostert, J. C., ... Franke, B. (2015). Lower white matter microstructure in the superior longitudinal fasciculus is associated with increased response time variability in adults with attention-deficit/hyperactivity disorder. *Journal of Psychiatry & Neuroscience, 40*, 344–351.